Transport Coefficients of Helical Wormlike Chains. 5. Translational Diffusion Coefficient of the Touched-Bead Model and Its Application to Oligo- and Polystyrenes

Takeshi Yamada, Takenao Yoshizaki, and Hiromi Yamakawa*

Department of Polymer Chemistry, Kyoto University, Kyoto 606-01, Japan

Received July 22, 1991

ABSTRACT: The translational diffusion coefficient D of the helical wormlike (HW) touched-bead model is evaluated theoretically by the use of the Kirkwood formula in the same spirit as in the evaluation of the intrinsic viscosity. The results are compared with those obtained previously on the basis of the HW cylinder model. Experimental results for D determined from dynamic light scattering measurements are also reported for 15 samples of atactic oligo- and polystyrenes (a-PS), each with the fraction of racemic diads $f_r = 0.59$, in the range of weight-average molecular weight M_w from 3.70×10^2 to 1.91×10^5 in cyclohexane at 34.5 °C (Θ). The agreement between the experimental and theoretical values is shown to be fairly good over the whole range of M_w down to the trimer, indicating that the Stokes(–Einstein) law holds even for an a-PS oligomer (nearly the trimer) corresponding to the single bead. This is in contrast to the previous result that its intrinsic viscosity is appreciably larger than the corresponding Einstein value. The HW model parameters determined from the present analysis are consistent with those from the mean-square optical anisotropy, mean-square radius of gyration, and intrinsic viscosity. Thus it is concluded that the HW model may give a consistent description of both the equilibrium and transport properties of unperturbed flexible polymer (and oligomer) chains.

I. Introduction

In previous papers, parts 1–3 of this series,[1-3] we evaluated the translational diffusion (or friction) coefficient D and the intrinsic viscosity $[\eta]$ of the helical wormlike (HW) chain[4-6] (without excluded volume) by an application of the Oseen–Burgers (OB) procedure of classical hydrodynamics[7] to the cylinder model. Interpolation formulas for both D and $[\eta]$ were also presented in parts 2 and 3, respectively. However, the one for $[\eta]$ cannot be applied to typical flexible polymers having in general the rather large ratio (~ 1) of the cylinder diameter d to the static stiffness parameter λ^{-1} of the HW chain, since it was constructed for $\lambda d \lesssim 0.08$. Recall that the numerical solution of the integral equation with the OB kernel cannot be obtained for such large λd (~ 1) when the ratio of the contour length L to λ^{-1} is small, while such a numerical difficulty never occurs in the evaluation of D if the Kirkwood formula[8,9] for D is employed, as done in part 2. In part 4,[10] therefore, we evaluated $[\eta]$ of the HW touched-bead model, for which the kernel does not cause the difficulty noted above, in order that we might apply the results to flexible polymers to explain the dependence of $[\eta]$ on the molecular weight M over its wide range (including the oligomer region) on the basis of the HW chain. Thus we desire to evaluate D for the same model for consistent treatments of D and $[\eta]$. One of the purposes of the present paper is to do this by the use of the Kirkwood formula.

On the other hand, we recently made experimental studies of $[\eta]$ for atactic polystyrene (a-PS) with the fraction of racemic diads $f_r = 0.59$,[11] atactic poly(methyl methacrylate) with $f_r = 0.79$,[12] and polyisobutylene[13] in respective Θ solvents. In all these cases, measurements were carried out over a wide range of M, including the oligomer region. From analyses of the data obtained on the basis of the HW touched-bead model,[10] it was found that the value of $[\eta]$ of an oligomer corresponding to the single bead does not always agree well with its Einstein intrinsic viscosity $[\eta]_E$, the values for the few lowest isobutylene oligomers even being negative. The value of $[\eta] > [\eta]_E$ for such an oligomer may be due to its nonspherical or elongated shape in solution[11] (or its rough surface), while the negative $[\eta]$ may be regarded as arising from specific interactions between solute and solvent molecules.[13] In any case, it is clear that classical hydrodynamics with the nonslip (or slip) boundary condition in general is not rigorously valid for small solute molecules in a shear flow. Thus it is interesting to examine whether the values of D for such oligomers can or cannot be explained by the Stokes(–Einstein) law. In this paper, therefore, we also report experimental data for D obtained for the a-PS in cyclohexane at 34.5 °C (Θ) as a first example of flexible polymers over a wide range of M, as always including the oligomer region, and analyze them by the use of the present HW theory for the touched-bead model. Although some experimental data for D for a-PS have already been reported,[14,15] no data are available for its oligomers with very low M.

In the Theoretical Section, we present basic equations required for the numerical calculation of D of the HW touched-bead model and compare the results with the previous ones for the cylinder model. Section III is the Experimental Section. In sections that follow, we present experimental results obtained from dynamic light scattering measurements and analyze the data obtained for D along the line mentioned above.

II. Theoretical Section

Basic Equations. Consider the HW touched-bead model[10] composed of N identical spherical beads of diameter d_b whose centers are located on the HW chain contour of total contour length L. The contour distance between two adjacent centers is set equal to the bead diameter d_b, so that

$$Nd_b = L \tag{1}$$

Thus the model is defined by the four model parameters: the constant curvature κ_0 and torsion τ_0 of the characteristic helix[4] of the HW chain, the static stiffness parameter λ^{-1}, and d_b, assuming that Poisson's ratio σ is zero, as usual. In the remainder of this section, all lengths are measured in units of λ^{-1}.

0024-9297/92/2225-0377$03.00/0 © 1992 American Chemical Society

According to the Kirkwood formula,[8,9] the translational diffusion coefficient D for this model may be written in the form

$$D = \frac{k_B T}{N\zeta_t}\left(1 + \frac{\zeta_t}{6\pi\eta_0 N}\sum_{\substack{p,q=1\\ p\neq q}}^{N}\langle R_{pq}^{-1}\rangle\right) \quad (2)$$

where k_B is the Boltzmann constant, T the absolute temperature, ζ_t the translational friction coefficient of the bead, η_0 the viscosity coefficient of the solvent, $\langle R_{pq}^{-1}\rangle$ the mean reciprocal distance between the centers of the pth and qth beads ($p, q = 1, 2, ..., N$), and we assume the Stokes formula for ζ_t, i.e.

$$\zeta_t = 3\pi\eta_0 d_b \quad (3)$$

For the chain without excluded volume, $\langle R_{pq}^{-1}\rangle$ is a function of $|p - q|$, i.e.

$$\langle R_{pq}^{-1}\rangle = \langle R^{-1}(|p - q|d_b)\rangle \quad (4)$$

where $\langle R^{-1}(s)\rangle$ is the mean reciprocal end-to-end distance of the HW chain of contour length s. With this relation, eq 2 may be reduced to

$$D = (k_B T/3\pi\eta_0 L) f_D(L;\kappa_0,\tau_0,d_b) \quad (5)$$

where the dimensionless function f_D is given by

$$f_D(L) = 1 + (d_b/L)\sum_{p=1}^{N-1}(L - pd_b)\langle R_{pq}^{-1}(pd_b)\rangle \qquad (N = L/d_b) \quad (6)$$

Note that we have used eqs 1 and 3 in the above reduction and that the function $f_D(L)$ depends on d_b and also on κ_0 and τ_0 through $\langle R^{-1}\rangle$.

An interpolation formula for $\langle R^{-1}(s)\rangle$ has already been given in the Appendix of ref 16, and it is convenient to reproduce it here. It reads

$$\langle R^{-1}(s)\rangle = [\langle R^2(s)\rangle_{KP}/\langle R^2(s)\rangle]^{1/2}\langle R^{-1}(s)\rangle_{KP}[1 + \kappa_0^2\Gamma(s)] \quad (7)$$

In eq 7, $\langle R^2(s)\rangle$ is the mean-square end-to-end distance of the HW chain of contour length s and is given by eq 54 of ref 6 (with $t = s$ and $\sigma = 0$)

$$\langle R^2(s)\rangle = c_\infty s - \frac{1}{2}\tau_0^2\nu^{-2} - 2\kappa_0^2\nu^{-2}(4 - \nu^2)(4 + \nu^2)^{-2} + e^{-2s}\left\{\frac{1}{2}\tau_0^2\nu^{-2} + 2\kappa_0^2\nu^{-2}(4 + \nu^2)^{-2}[(4 - \nu^2)\cos\nu s - 4\nu\sin\nu s]\right\} \quad (8)$$

with

$$c_\infty = (4 + \tau_0^2)/(4 + \kappa_0^2 + \tau_0^2) \quad (9)$$

$$\nu = (\kappa_0^2 + \tau_0^2)^{1/2} \quad (10)$$

$\langle R^2(s)\rangle_{KP}$ is the mean-square end-to-end distance of the Kratky–Porod (KP) wormlike chain of the same contour length and is given by eq 8 with $\kappa_0 = 0$ ($c_\infty = 1$ and $\nu = \tau_0$). $\langle R^{-1}(s)\rangle_{KP}$ is the mean reciprocal distance of the same KP chain and is given approximately by[7]

$$\langle R^{-1}(s)\rangle_{KP} = \left(\frac{6}{\pi s}\right)^{1/2}\left(1 - \frac{1}{40s} - \frac{73}{4480s^2}\right) \quad \text{for } s > 2.278$$

$$= s^{-1}\left(1 + \frac{1}{3}s + 0.1130s^2 - 0.02447s^3\right) \quad \text{for } s \le 2.278 \quad (11)$$

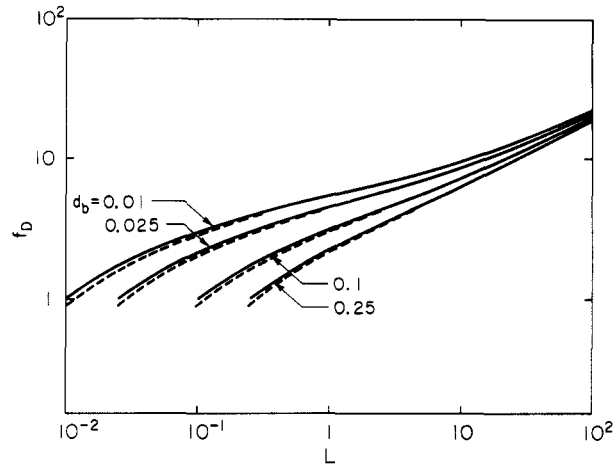

Figure 1. Double-logarithmic plots of f_D against L for the KP chain with $d_b = 0.01$, 0.025, 0.1, and 0.25. The solid and dashed curves represent the values for the touched-bead model and the corresponding cylinder model with $d = 0.891 d_b$, respectively (see the text).

The function $\Gamma(s)$ is given by

$$\Gamma(s) = \exp(-2/s)\sum_{k=1}^{2}A_k s^{-k} + \exp\left[-\left(2 + \frac{3}{4}\nu\right)s\right]\sum_{k=3}^{7}A_k s^k \quad (12)$$

with

$$A_1 = 3(4 + \tau_0^2)^{-1}(4 + \nu^2)^{-1} - \frac{3}{10}(9 + \nu^2)^{-1}(36 + \nu^2)^{-1}[1 + (101 + \kappa_0^2)(4 + \tau_0^2)^{-1} + 3(160 + 7\kappa_0^2)(4 + \tau_0^2)^{-2}] \quad (13)$$

$$A_k = \{1 + \delta_{k2}[(4 + \nu^2)^{-1} - 1]\}\sum_{i=0}^{7}\sum_{j=0}^{6}a_{ij}^k\nu^i(\tau_0/\nu)^{2j} \qquad (k = 2\text{–}7) \quad (14)$$

where δ_{ij} is the Kronecker delta and a_{ij}^k are the numerical coefficients independent of s, κ_0, and τ_0, their values being given in Table II of ref 16.

The application of the above formulas with the values of a_{ij}^k given in Table II of ref 16 is restricted to the following ranges of κ_0 and τ_0: the shaded domain in Figure 3 of ref 2; $\nu \le 1.5$ and $0 \le \tau_0/\nu \le 0.5$; and $\nu \le 8$ and $0.5 \le \tau_0/\nu \le 1$. For other values of κ_0 and τ_0, we must evaluate the coefficients A_k ($k = 2$–7) by the use of the numerical results for $\langle R^{-1}(s)\rangle$ calculated by the procedure described in ref 17. For some interesting cases of κ_0 and τ_0, the values of A_k ($k = 2$–7) thus determined are given in Appendix B of ref 18. Finally, we note that the above interpolation formula with $A_k = 0$ ($k = 2$–7) gives a very good approximation for $\nu \gtrsim 20$.

Numerical Results. Now we examine the behavior of the function f_D for the HW touched-bead model on the basis of the values calculated from eq 6 with eqs 7–14. All numerical work has been done by the use of a FACOM M-780 digital computer in this university.

Figure 1 shows double-logarithmic plots of f_D against L for the KP chain ($\kappa_0 = 0$) with various values of d_b. As noted in part 2,[2] for the HW chain of weak helical nature, i.e., for $\tau_0/\nu \gtrsim 0.5$, the difference between the HW and (associated) KP chains in the dependence of D (or f_D) on L is negligibly small. Thus the numerical results displayed in Figure 1 may be considered to apply approximately to chains of weak helical nature such as a-PS, for which the parameters κ_0 and τ_0 have already been determined to be 3.0 and 6.0, respectively.[19] [Recall that the interpolation formula given in part 2 does not cover such a region of (κ_0,

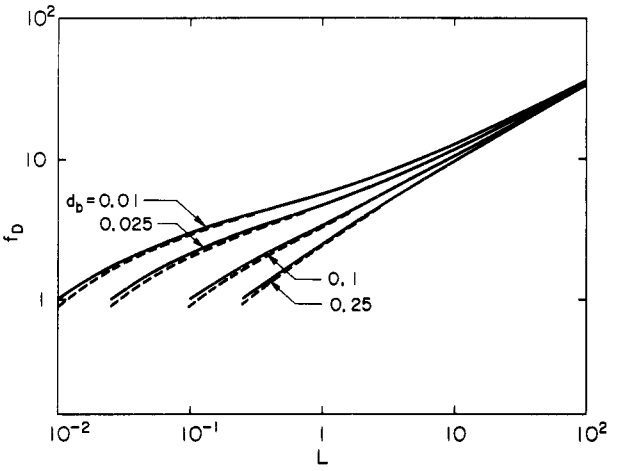

Figure 2. Double-logarithmic plots of f_D against L for the case of $\kappa_0 = 4.5$ and $\tau_0 = 2.0$ [atactic poly(methyl methacrylate)] with $d_b = 0.01$, 0.025, 0.1, and 0.25. See legend for Figure 1.

τ_0).] Figure 2 shows similar plots for the case of atactic poly(methyl methacrylate) (a-PMMA) with $f_r = 0.79$, as an example of chains of strong helical nature, whose HW model parameters κ_0 and τ_0 determined from an analysis of $[\eta]$[12] are 4.5 and 2.0, respectively. In both figures, the solid curves represent the present theoretical values for the touched-bead model. For comparison, the values for the HW cylinder model (dashed curves) calculated from the interpolation formula given in part 2 are also plotted in the figures. We note that f_D is equivalent to the function $\bar{s}$ defined in part 2, and that we have used the values of the diameter d for the corresponding cylinder model computed from the relation $d = 0.891 d_b$.[20] This relation was obtained from a comparison of theoretical values for the touched-bead rod and the straight cylinder with hemisphere caps on both terminal ends.

From these figures, it is seen that the values of D for the two models differ appreciably from each other for short chains even with the above relation between d and d_b. Therefore, we should use the same model, especially the touched-bead model for flexible chains, when we analyze data for D and $[\eta]$ consistently over a wide range of M. In fact, the interpolation formula for $[\eta]$ for the cylinder model is not applicable to (very) flexible chains in the oligomer region.

III. Experimental Section

Materials. Most of the a-PS samples used in this work are the same as those used in the previous studies of the mean-square optical anisotropy $\langle\Gamma^2\rangle$,[19] $[\eta]$,[11] the mean-square radius of gyration $\langle S^2\rangle$,[21] and the transport factors ρ and Φ for long flexible chains,[22] i.e., the fractions separated by gel permeation chromatography (GPC) or fractional precipitation from the original standard samples supplied from Tosoh Co., Ltd. They are sufficiently narrow in molecular weight distribution and have fixed stereochemical composition f_r independent of molecular weight. The values of the weight-average molecular weight M_w obtained from analytical GPC ($M_w < 10^3$) and light scattering measurements ($M_w > 10^3$) are given in Table I along with those of the ratio of M_w to the number-average molecular weight M_n. The values for the additional sample F20[23] are also given in Table I.

The solvent cyclohexane used for dynamic light scattering (DLS) measurements was purified according to a standard procedure.

Dynamic Light Scattering. DLS measurements were carried out to determine D for the 15 a-PS samples OS3 through F20 except for F40, F80, and F128-2 in cyclohexane at 34.5 °C by the use of a Brookhaven Instruments Model BI-200SM light scattering goniometer with vertically polarized incident light of 488-nm wavelength from a Spectra-Physics Model 2020 argon ion laser equipped with a Model 583 temperature-stabilized etalon for single-frequency-mode operation. The photomultiplier tube used was an EMI 9863B/350, the output of which was processed by a Brookhaven Instruments Model BI2030AT autocorrelator with 264 channels. A minor modification has been made of the detector alignment.[22] The normalized autocorrelation function $g^{(2)}(t)$ of scattered light intensity $I(t)$, i.e.

$$g^{(2)}(t) = \langle I(0)I(t)\rangle/\langle I(0)\rangle^2 \tag{15}$$

was measured at four or five different concentrations and at scattering angles ranging from 15 to 110°. The relaxation rate of $g^{(2)}(t) - 1$ increases with decreasing M_w, so that the sampling time must be properly chosen depending on M_w. The details are given in the next section.

The most concentrated cyclohexane solutions of the samples were prepared by continuous stirring in the dark at ca. 50 °C for 1 day. Although the present stirring time was shorter than before,[21] complete dissolution of each polymer sample was confirmed from flow times for the highest F20 of the samples used in the present measurements. These solutions were optically purified by filtration through a Teflon membrane of 0.1-μm pore size. (From flow times, the filtration was confirmed to cause neither change in polymer concentration nor chain scission.) All solutions of lower concentrations were obtained by sequential dilution. The weight concentrations of test solutions were determined gravimetrically and converted to mass concentrations c by the use of the densities of the solutions.

From the data for $g^{(2)}(t)$, we determined the diffusion coefficient $D(\infty)$ at an infinitely long time in almost the same manner as used in the previous work.[22] $g^{(2)}(t)$ at infinite dilution is related to the dynamic structure factor $S(k,t)$ by the equation

$$\ln [g^{(2)}(t) - 1] = \text{const} + \ln [S(k,t)/S(k,0)] \tag{16}$$

where k is the magnitude of the scattering vector and is given by

$$k = (4\pi/\tilde{\lambda}) \sin (\theta/2) \tag{17}$$

with θ the scattering angle and $\tilde{\lambda}$ the wavelength of the incident light in the solvent. The second term on the right-hand side of eq 16 may be written in the form

$$\ln [S(k,t)/S(k,0)] = -k^2 t D(t)[1 + O(k^2)] \tag{18}$$

At such a long time t that all the internal motions relax away and $D(t)$ becomes a constant $D(\infty)$, eq 16 with eq 18 may then be rewritten in the form

$$\ln [g^{(2)}(t) - 1] = \text{const} - At \tag{19}$$

An equation similar to eq 19 holds at finite concentrations c unless c is large. Thus the apparent diffusion coefficient $D^{(LS)}(c)$ determined from DLS measurements at finite c may be evaluated from

$$D^{(LS)}(c) = \lim_{k\to 0} A/k^2 \tag{20}$$

At sufficiently low concentrations, $D^{(LS)}(c)$ may be expanded as

$$D^{(LS)}(c) = D^{(LS)}(0)(1 + k_D^{(LS)} c + \ldots) \tag{21}$$

so that the desired $D(\infty)$ may be determined from extrapolation

Table I
Values of M_w and M_w/M_n for Atactic Oligo- and Polystyrenes with $f_r = 0.59$ in Cyclohexane at 34.5 °C

sample	M_w	M_w/M_n	sample	M_w	M_w/M_n
OS3	3.70×10^2	1.00	F1-2	1.01×10^4	1.03
OS4	4.74×10^2	1.00	F2	2.05×10^4	1.02
OS5	5.78×10^2	1.00	F4	4.00×10^4	1.02
OS6	6.80×10^2	1.00	F10	9.73×10^4	1.02
OS8	9.04×10^2	1.01	F20	1.91×10^5	1.02
A1000-b	1.48×10^3	1.02	F40	3.59×10^5	1.01
A2500-a′	1.78×10^3	1.04	F80	7.32×10^5	1.01
A2500-a	2.27×10^3	1.05	F128-2	1.32×10^6	1.05
A2500-b	3.48×10^3	1.07			
A5000-3	5.38×10^3	1.03			

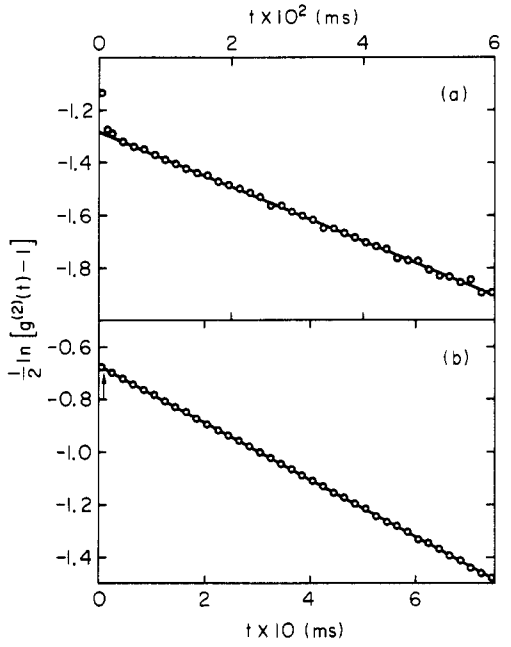

Figure 3. Plots of $(1/2)$ ln $[g^{(2)}(t) - 1]$ against t for the a-PS samples OS3 ($c = 3.12 \times 10^{-1}$ g/cm^3, $\theta = 15°$) (a) and F20 ($c = 6.59 \times 10^{-3}$ g/cm^3, $\theta = 20°$) (b) in cyclohexane at 34.5 °C. The arrow in case b indicates the value of $t = 10\tau_1$, and the straight lines have the respective slopes of $-A$.

of $D^{(LS)}(c)$ to $c = 0$

$$D(\infty) \equiv D = D^{(LS)}(0) \tag{22}$$

Note that the coefficient $k_D^{(LS)}$ defined in eq 21 is not equivalent to the coefficient k_D appearing in the ordinary diffusion or sedimentation equation (see eq 30.40 of ref 9).

The values of the refractive index at a wavelength of 488 nm and viscosity coefficient η_0 that we used for cyclohexane at 34.5 °C are 1.424 and 0.768 cP, respectively.

IV. Experimental Results

Figure 3 shows plots of $(1/2)$ ln $[g^{(2)}(t) - 1]$ against t for the data for the a-PS samples OS3 (a) and F20 (b) in cyclohexane at 34.5 °C, which were obtained at the respective highest concentrations c and at the respective smallest scattering angles θ; i.e., $c = 3.12 \times 10^{-1}$ g/cm^3 and $\theta = 15°$ for the former and $c = 6.59 \times 10^{-3}$ g/cm^3 and $\theta = 20°$ for the latter. In general, the relaxation rate k^2D of $g^{(2)}(t) - 1$ increased with decreasing M_w and with increasing k (or θ), so that the sampling time was shortened as M_w was decreased and as θ was increased, but we always made it larger than 0.3 μs. The sampling times adopted in obtaining the data in Figure 3a and b were 0.8 and 10 μs, respectively.

As in the previous study of ρ and Φ,[22] we adopted the data for t larger than the time $10\tau_1$ for the determination of $D(\infty)$, where τ_1 is the relaxation time of the first normal mode for the Gaussian chain (the spring-bead model) and is given in the nondraining limit by[9,24]

$$\tau_1 = M\eta_0[\eta]/0.586RT\lambda_1 \tag{23}$$

with R the gas constant and λ_1 (=4.04) the corresponding reduced Zimm eigenvalue.[9,25] In Figure 3b, the arrow indicates the value of $t = 10\tau_1$. However, the value 8.9 μs of $10\tau_1$ for the sample F20 is much smaller than the corresponding value of 68 μs for the sample F80 studied previously,[22] and the tendency for the plot to be slightly concave upward for $t < 10\tau_1$, as observed for the sample F80 (see Figure 2 of ref 22), is not very clearly seen in Figure 3b. Further, for the samples with small M_w (<2 × 10^4), the time $10\tau_1$ becomes smaller than the sampling time actually adopted, and therefore, the above criterion makes no sense for such samples. As seen from Figure 3a, however, the plot is concave upward for very small t (<1 μs). This may probably be due to the afterpulsing in the photomultiplier tube and may be considered to have nothing to do with the time dependence of D discussed above. Thus we may neglect such data points in the determination of the slope $-A$.

The intensity of scattered light (or number of scattered photons per second) is very weak for the oligomer samples. As a result, the data for the sample OS3 scatter more appreciably than those for F20, as seen from the figure.

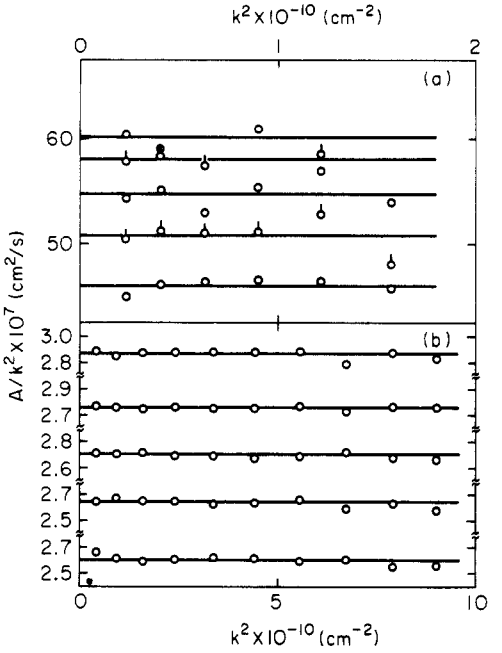

Figure 4. Plots of A/k^2 against k^2 for the a-PS samples OS3 (a) and F20 (b) in cyclohexane at 34.5 °C. The polymer mass concentrations c are 1.07×10^{-1}, 1.35×10^{-1}, 1.85×10^{-1}, 2.31×10^{-1}, and 3.12×10^{-1} g/cm^3 for case a and 2.70×10^{-3}, 3.99×10^{-3}, 5.01×10^{-3}, 5.98×10^{-3}, and 6.59×10^{-3} g/cm^3 for case b from top to bottom.

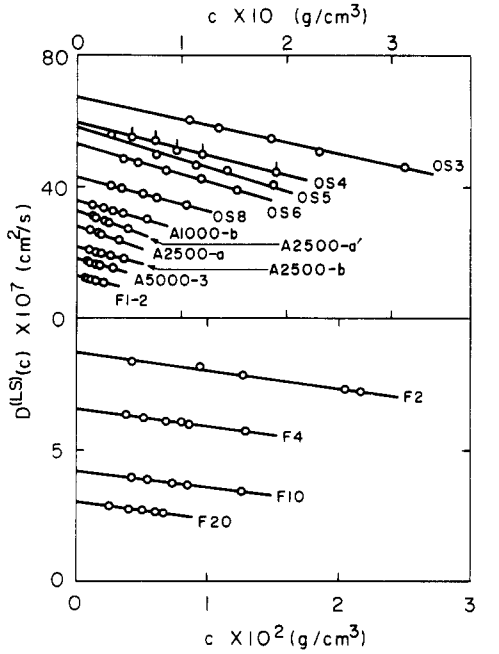

Figure 5. Plots of $D^{(LS)}(c)$ against c for the a-PS samples indicated in cyclohexane at 34.5 °C.

Table II
Results of DLS Measurements on Atactic Oligo- and Polystyrenes with f_r = 0.59 in Cyclohexane at 34.5 °C

sample	10^7D, cm²/s	$k_D^{(LS)}$, cm³/g	sample	10^7D, cm²/s	$k_D^{(LS)}$, cm³/g
OS3	67.4	-1.0_3	F1-2	13.0	-6.0_7
OS4	59.6	-1.3_5	F2	8.74	-7.9_4
OS5	58.2	-1.6_7	F4	6.58	$-10._0$
OS6	53.3	-1.7_5	F10	4.21	$-14._8$
OS8	43.1	-1.9_1	F20	3.0_4	$-21._7$
A1000-b	35.9	-2.5_2	F40[a]	2.25	$-28._9$
A2500-a′	32.9	-3.4_5	F80	1.57	$-38._9$
A2500-a	28.2	-3.8_0	F128-2	1.17	$-68._4$
A2500-b	21.7	-3.7_8			
A5000-3	18.2	-4.7_2			

[a] The values of D of F40, F80, and F128-2 have been reproduced from ref 22.

Figure 6. Double-logarithmic plots of $\eta_0 DM_w/k_BT$ against M_w for a-PS in cyclohexane at 34.5 °C: ○, present data; ●, previous data[22]; △, data by Huber et al.[15] The dotted straight line has a slope of 0.5.

The relative errors in the slopes $-A$ (of the straight lines) determined by the method of least squares from the data shown in Figure 3a and b were determined to be ±3% and ±0.5%, respectively.

Figure 4 shows plots of the values of A/k^2 thus determined against k^2 for the same samples OS3 (a) and F20 (b) in cyclohexane at 34.5 °C, the points representing the values at $c = 1.07 \times 10^{-1}$, 1.35×10^{-1}, 1.85×10^{-1}, 2.31×10^{-1}, and 3.12×10^{-1} g/cm³ for OS3 and at $c = 2.70 \times 10^{-3}$, 3.99×10^{-3}, 5.01×10^{-3}, 5.98×10^{-3}, and 6.59×10^{-3} g/cm³ for F20 from top to bottom. In the range of k^2 displayed, A/k^2 is seen to be almost independent of k, so that we adopt as the value of $D^{(LS)}(c)$ $[=(A/k^2)_{k=0}]$ at each finite c the mean value represented by the horizontal line. Figure 5 shows plots of the values of $D^{(LS)}(c)$ thus determined against c for the 15 a-PS samples indicated in cyclohexane at 34.5 °C, which are seen to follow straight lines. We may then determine $D(0)$ $(=D)$ and $k_D^{(LS)}$ for each sample from the ordinate intercept and slope of each of them.

The values of D and $k_D^{(LS)}$ obtained are given in Table II. The values of D for the three samples with the highest M_w, i.e., F40, F80, and F128-2, have been reproduced from ref 22, and those of $k_D^{(LS)}$ for these samples are the ones determined there (although not reported). The possible relative errors in D were estimated to be ±1% for $M_w \gtrsim 10^5$, ±1.5% for $10^4 \lesssim M_w \lesssim 10^5$, ±2% for $3 \times 10^3 \lesssim M_w \lesssim 10^4$, ±3% for $10^3 \lesssim M_w \lesssim 3 \times 10^3$, and ±5% for $M_w \lesssim 10^3$. The present results for $k_D^{(LS)}$ are in good agreement with those by Huber et al.[15] for $M_w < 3 \times 10^4$, and the sign of $k_D^{(LS)}$ is consistent with the theoretical prediction[9] for k_D (appearing in the ordinary diffusion or sedimentation equation) for the Gaussian chain. However, these two coefficients are not equivalent to each other since $D^{(LS)}(c)$ represents a kind of relaxation rate of the segment-density fluctuation and cannot be directly related to the so-called self-diffusion coefficient except at infinite dilution.[26] Further, they have not been evaluated theoretically for short chains. Thus we do not analyze the present data for $k_D^{(LS)}$.

Figure 6 shows double-logarithmic plots of $\eta_0 DM_w/k_BT$ (in cm⁻¹) against M_w for the present (unfilled circles) and previous (filled circles) data for the a-PS in cyclohexane at 34.5 °C. (Note that the quantity $\eta_0 DM_w/k_BT$ is proportional to the sedimentation coefficient.) The solid curve connects these data points smoothly, and the dotted line indicates its asymptotic straight line of slope 1/2. The data points slightly deviate upward from this straight line for $5 \times 10^2 < M_w < 2.5 \times 10^3$. For comparison, the data by Huber et al.[15] (unfilled triangles) for a-PS in cyclohexane at 34.5 °C are also plotted in Figure 6. Their data points are somewhat lower than ours.

V. Discussion

Analysis of Experimental Data. In this section, all lengths are unreduced unless otherwise noted. From eq 5, the quantity $\eta_0 DM_w/k_BT$ may then be written in the form

$$\eta_0 DM_w/k_BT = (M_L/3\pi) f_D(\lambda L; \lambda^{-1}\kappa_0, \lambda^{-1}\tau_0, \lambda d_b) \quad (24)$$

where M_L is the shift factor as defined as the molecular weight per unit contour length, and the function f_D is given by eq 6 and evaluated numerically. Corresponding to the analysis of $[\eta]$,[11-13] we analyze the data by the use of the equations

$$\log (\eta_0 DM_w/k_BT) = \log f_D(\lambda L) + \log M_L - 0.975 \quad (25)$$

$$\log M_w = \log (\lambda L) + \log (\lambda^{-1} M_L) \quad (26)$$

The quantities M_L and $\lambda^{-1}M_L$ (and therefore λ^{-1} and M_L) may be estimated from a best fit of double-logarithmic plots of the theoretical f_D against λL for properly chosen values of $\lambda^{-1}\kappa_0$, $\lambda^{-1}\tau_0$, and λd_b to that of the observed $\eta_0 DM_w/k_BT$ against M_w, so that we may in principle determine $\lambda^{-1}\kappa_0$, $\lambda^{-1}\tau_0$, λ^{-1}, M_L, and d_b. As in the case of $[\eta]$ for a-PS,[11] however, it is difficult to determine all of the five model parameters in this manner, since the double-logarithmic plot of $\eta_0 DM_w/k_BT$ against M_w deviates only slightly from the straight line of slope 1/2 and does not exhibit remarkable inflection as observed in the case of $[\eta]$ for a-PMMA.[12] Thus, in this paper, we assume that $\lambda^{-1}\kappa_0$ and $\lambda^{-1}\tau_0$ are the same as those estimated previously[19] from the analysis of the data for $\langle\Gamma^2\rangle$ in cyclohexane at 34.5 °C, i.e., $\lambda^{-1}\kappa_0 = 3.0$ and $\lambda^{-1}\tau_0 = 6.0$, and determine the remaining three parameters λ^{-1}, M_L, and d_b.

Figure 7 shows double-logarithmic plots of $\eta_0 DM_w/k_BT$ against M_w for the a-PS in cyclohexane at 34.5 °C. The unfilled circles represent the present and previous[22] experimental values, and the solid curve represents the best-fit theoretical values for $N \geq 2$ calculated from eq 6 with $\lambda d_b = 0.35$, $\log M_L = 9.544$, and $\log(\lambda^{-1} M_L) = 2.975$, the dashed line segment connecting those values for $N = 1$ and 2. The dotted line indicates an asymptotic straight line of slope 1/2. The values of the HW model parameters thus determined are listed in the first row of Table III along with those determined from analyses of $\langle\Gamma^2\rangle$, $\langle S^2\rangle$, and $[\eta]$ for the same system.

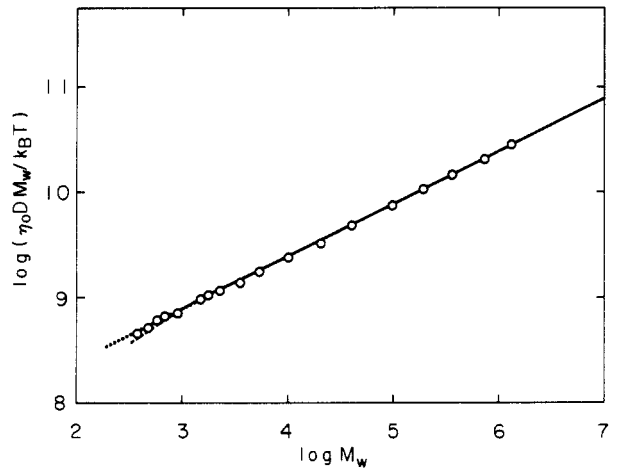

Figure 7. Comparison between the observed and theoretical values of $\eta_0 D M_w/k_B T$ for the a-PS in cyclohexane at 34.5 °C. The solid curve represents the best-fit HW theoretical values for $N \geq 2$, the dashed line segment connecting the values for $N = 1$ and 2. The dotted straight line has a slope of 0.5.

Table III
Values of the HW Model Parameters for Atactic Polystyrenes with $f_r = 0.59$ in Cyclohexane at 34.5 °C

$\lambda^{-1}\kappa_0$	$\lambda^{-1}\tau_0$	λ^{-1}, Å	M_L, Å^{-1}	d_b, Å	obsd quantity
(3.0)	(6.0)	27.0	35.0	9.5	D
3.0	6.0	22.7	37.1		$\langle\Gamma^2\rangle$
(3.0)	(6.0)	22.5	36.7		$\langle S^2\rangle$
(3.0)	(6.0)	23.5	42.6	10.1	$[\eta]$

As seen in Figure 7, the agreement between the experimental and theoretical values of D is fairly good over the whole range of M_w. Although the value 9.5 Å of d_b is in good agreement with the value 10.1 Å determined from $[\eta]$, the agreement between the experimental and theoretical values for the latter is not as good as for the present case for $M_w \lesssim 10^3$; the experimental values of $[\eta]$ are appreciably larger than the theoretical ones in this range of M_w (see Figure 3 of ref 11). As already mentioned in ref 11 and in the Introduction, the oligomer corresponding to the single bead may be considered to take a nonspherical or elongated shape in solution on statistical average. Thus the difference between D and $[\eta]$ in the agreement between theory and experiment in such an oligomer region may be regarded as arising from the fact that the effect of the deviation from an ideal spherical shape is more remarkable on $[\eta]$ than on D (or the translational friction coefficient). The present values of the model parameters λ^{-1} and M_L given in Table III are also somewhat different from those determined from other observed quantities. The reason for this is discussed in the next subsection.

Dependence of ρ on M_w. In the previous study of $\langle S^2\rangle$,[21] we examined the dependence on M_w of the Flory–Fox factor Φ, now defined as the ratio of the (molar) hydrodynamic volume defined from $[\eta]$ to $\langle S^2\rangle^{3/2}$. Another interesting dimensionless transport factor is the ratio ρ defined as

$$\rho = \langle S^2\rangle^{1/2}/R_H \tag{27}$$

where R_H is the hydrodynamic radius defined from D as

$$R_H = k_B T/6\pi\eta_0 D \tag{28}$$

In Table IV are given the values of $\langle S^2\rangle^{1/2}$ determined previously from small-angle X-ray and light scattering measurements,[21,22] those of R_H calculated from eq 28 with the values of D given in Table II, and those of ρ calculated from eq 27 with them. The coil limiting value ρ_∞ of ρ has been calculated to be 1.28 as the mean of the values of ρ for the three highest samples F40, F80, and F128-2, which is in good agreement with the value of 1.28 determined by Schmidt and Burchard for the same system,[14] as noted previously.[22] We note that the values of ρ (and ρ_∞) are not very much affected by the polydispersity, its correction changing the value of ρ_∞ only from 1.28 to 1.26.[22]

Table IV
Values of $\langle S^2\rangle^{1/2}$, R_H, and ρ for Atactic Oligo- and Polystyrenes with $f_r = 0.59$ in Cyclohexane at 34.5 °C

sample	$\langle S^2\rangle^{1/2}$, Å	R_H, Å	ρ
OS3		4.3_5	
OS4		4.9_2	
OS5	3.3_9	5.0_4	0.67_2
OS6	3.9_2	5.5_1	0.71_2
OS8	4.8_7	6.8_1	0.71_5
A1000-b	7.9_9	8.1_8	0.97_7
A2500-a′	9.4_2	8.9_2	1.0_6
A2500-a	$11._2$	$10._4$	1.0_8
A2500-b	$14._6$	$13._5$	1.0_8
A5000-3	$19._0$	$16._1$	1.1_8
F1-2	$27._3$	$22._6$	1.2_1
F2	$39._7$	$33._6$	1.1_8
F4	$56._6$	$44._6$	1.2_7
F10	$91._0$	$69._7$	1.3_1
F20		$96._9$	
F40	16_7	13_0	1.2_8
F80	24_0	18_7	1.2_8
F128-2	31_9	25_1	1.2_8

Now we calculate the HW theoretical values of ρ. This also requires the theoretical expression for $\langle S^2\rangle$. For the HW chain of total contour length L, it is given by[4-6]

$$\langle S^2\rangle = \lambda^{-2} f_S(\lambda L; \lambda^{-1}\kappa_0, \lambda^{-1}\tau_0) \tag{29}$$

where the function f_S is defined by

$$f_S(L;\kappa_0,\tau_0) = \frac{\tau_0^2}{\nu^2} f_{S,KP}(L) + \frac{\kappa_0^2}{\nu^2}\left[\frac{L}{3r}\cos\phi - \frac{1}{r^2}\cos(2\phi) + \frac{2}{r^3 L}\cos(3\phi) - \frac{2}{r^4 L^2}\cos(4\phi) + \frac{2}{r^4 L^2}e^{-2L}\cos(\nu L + 4\phi)\right] \tag{30}$$

with

$$r = (4 + \nu^2)^{1/2} \tag{31}$$

$$\phi = \cos^{-1}(2/r) \tag{32}$$

$$f_{S,KP}(L) = \frac{L}{6} - \frac{1}{4} + \frac{1}{4L} - \frac{1}{8L^2}(1 - e^{-2L}) \tag{33}$$

and with ν being given by eq 10 (in units of λ^{-1}). The theoretical value of ρ_∞ calculated from eq 27 with eqs 5 and 29 is 1.505, which is ca. 18% larger than the experimental value 1.28. This is due to the fact that the Kirkwood formula gives the translational diffusion coefficient of the center of mass of the polymer chain at $t = 0$, which is larger than $D(\infty)$.[27] This is also the main reason for the differences between the values of the HW model parameters λ^{-1} and M_L from D and $\langle S^2\rangle$ (see Table III). (Note that the differences between the values of λ^{-1} and M_L from $[\eta]$ and $\langle S^2\rangle$ are mainly due to the fact that the HW theory of $[\eta]$[10] in the Kirkwood–Riseman scheme[9] also overestimates Φ in the coil limit.) Thus, for a comparison between theory and experiment with respect to the dependence of ρ on M_w, we consider the ratio ρ/ρ_∞, for convenience.

Figure 8 shows double-logarithmic plots of ρ/ρ_∞ against M_w. The unfilled circles represent the experimental values,

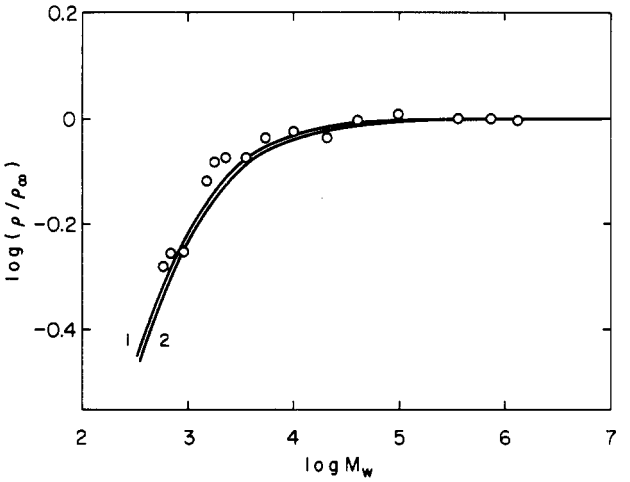

Figure 8. Molecular weight dependence of ρ reduced with ρ_∞ for the a-PS with $f_r = 0.59$ in cyclohexane at 34.5 °C. The solid curves represent the HW theoretical values calculated with $\lambda^{-1}\kappa_0 = 3.0$, $\lambda^{-1}\tau_0 = 6.0$, $\lambda^{-1} = 27.0$ Å, $M_L = 35.0$ Å^{-1}, and $d_b = 9.5$ Å (1) and $\lambda^{-1}\kappa_0 = 3.0$, $\lambda^{-1}\tau_0 = 6.0$, $\lambda^{-1} = 22.5$ Å, $M_L = 36.7$ Å^{-1}, and $d_b = 9.5$ Å (2).

and the solid curves 1 and 2 represent the HW theoretical values with the sets of the model parameters: $\lambda^{-1}\kappa_0 = 3.0$, $\lambda^{-1}\tau_0 = 6.0$, $\lambda^{-1} = 27.0$ Å, and $M_L = 35.0$ Å^{-1} from D, and $\lambda^{-1}\kappa_0 = 3.0$, $\lambda^{-1}\tau_0 = 6.0$, $\lambda^{-1} = 22.5$ Å, and $M_L = 36.7$ Å^{-1} from $\langle S^2\rangle$, respectively, with $d_b = 9.5$ Å from D for both cases. As in the case of Φ/Φ_∞,[21] the observed ρ/ρ_∞ is essentially constant for $M_w > 10^5$, but in contrast to that case, it steeply decreases as M_w is decreased from 10^5. Note that this decrease in ρ/ρ_∞ at small M_w is due to the decrease in the ratio $\langle S^2\rangle/M_w$. It is seen that the theory can explain such behavior almost quantitatively; and thus the HW theory may well explain consistently the behavior of D and $\langle S^2\rangle$ over the whole range of M_w (except for the absolute value of ρ_∞).

VI. Conclusion

We have evaluated theoretically the translational diffusion coefficient D of the HW touched-bead model by the use of the Kirkwood formula. On the basis of its theoretical values, we have also analyzed the present experimental data for D for a-PS with $f_r = 0.59$ in cyclohexane at 34.5 °C (Θ) to show that the HW theory may well explain its behavior over a wide range of M_w down to the trimer (corresponding nearly to the single bead). The values of the HW model parameters λ^{-1} and M_L determined from D, $[\eta]$, and the equilibrium properties $\langle\Gamma^2\rangle$ and $\langle S^2\rangle$ have been found to be somewhat different from each other. (Recall that the parameters $\lambda^{-1}\kappa_0$ and $\lambda^{-1}\tau_0$ are assumed to take the same values as those determined from $\langle\Gamma^2\rangle$.) These slight differences between the parameter values from the different properties are mainly due to the incompleteness of the polymer transport theory (both of D and $[\eta]$) with the preaveraged hydrodynamic interaction tensor. Thus we may conclude that on the whole the HW model may explain consistently the behavior of all equilibrium and transport properties, including the scattering function,[28] for a-PS. Indeed, to examine such validity of the model was the primary purpose of this series of experimental studies of dilute solution properties of a-PS in the Θ solvent.

It has been found that the value of $[\eta]$ of an a-PS oligomer corresponding to the single bead is appreciably larger than its Einstein intrinsic viscosity,[11] while the Stokes(–Einstein) law holds rather well for the same oligomer. An inconsistency of this kind may be resolved within the framework of classical hydrodynamics, considering the fact that such an oligomer takes a nonspherical or elongated shape in solution, as already mentioned. However, as reported previously,[13] there exist those polymer–solvent systems such as polyisobutylene in isoamyl isovalerate and in benzene in which $[\eta]$ becomes negative for the oligomers, and there is no promise that we can make classical hydrodynamic treatments of them. Thus it is very interesting to explore the behavior of D for such systems. This is the problem in our forthcoming papers.

Acknowledgment. This research was supported by a Grant-in-Aid (01430018) from the Ministry of Education, Science, and Culture, Japan.

References and Notes

(1) Yamakawa, H.; Yoshizaki, T.; Fujii, M. *Macromolecules* **1977**, *10*, 934.
(2) Yamakawa, H.; Yoshizaki, T. *Macromolecules* **1979**, *12*, 32.
(3) Yamakawa, H.; Yoshizaki, T. *Macromolecules* **1980**, *13*, 633.
(4) Yamakawa, H. *Annu. Rev. Phys. Chem.* **1984**, *35*, 23.
(5) Yamakawa, H. In *Molecular Conformation and Dynamics of Macromolecules in Condensed Systems*; Nagasawa, M. Ed.; Elsevier: Amsterdam, 1988; p 21.
(6) Yamakawa, H.; Fujii, M. *J. Chem. Phys.* **1976**, *64*, 5222.
(7) Yamakawa, H.; Fujii, M. *Macromolecules* **1973**, *6*, 407.
(8) Kirkwood, J. G. *Recl. Trav. Chim.* **1949**, *68*, 649; *J. Polym. Sci.* **1954**, *12*, 1.
(9) Yamakawa, H. *Modern Theory of Polymer Solutions*; Harper & Row: New York, 1971.
(10) Yoshizaki, T.; Nitta, I.; Yamakawa, H. *Macromolecules* **1988**, *21*, 165.
(11) Einaga, Y.; Koyama, H.; Konishi, T.; Yamakawa, H. *Macromolecules* **1989**, *22*, 3419.
(12) Fujii, Y.; Tamai, Y.; Konishi, T.; Yamakawa, H. *Macromolecules* **1991**, *24*, 1608.
(13) Abe, F.; Einaga, Y.; Yamakawa, H. *Macromolecules* **1991**, *24*, 4423.
(14) Schmidt, M.; Burchard, W. *Macromolecules* **1981**, *14*, 210, and references cited therein.
(15) Huber, K.; Bantle, S.; Lutz, P.; Burchard, W. *Macromolecules* **1985**, *18*, 1461.
(16) Yamakawa, H.; Yoshizaki, T. *J. Chem. Phys.* **1983**, *78*, 572.
(17) Yamakawa, H.; Shimada, J.; Fujii, M. *J. Chem. Phys.* **1978**, *68*, 2140.
(18) Yamakawa, H.; Yoshizaki, T.; Fujii, M. *J. Chem. Phys.* **1986**, *84*, 4693.
(19) Konishi, T.; Yoshizaki, T.; Shimada, J.; Yamakawa, H. *Macromolecules* **1989**, *22*, 1921.
(20) Yamakawa, H. *Macromolecules* **1983**, *16*, 1928.
(21) Konishi, T.; Yoshizaki, T.; Saito, T.; Einaga, Y.; Yamakawa, H. *Macromolecules* **1990**, *23*, 290.
(22) Konishi, T.; Yoshizaki, T.; Yamakawa, H. *Macromolecules* **1991**, *24*, 5614.
(23) Abe, F.; Einaga, Y.; Yoshizaki, T.; Yamakawa, H. *Macromolecules*, to be submitted.
(24) Zimm, B. H. *J. Chem. Phys.* **1956**, *24*, 269.
(25) Zimm, B. H.; Roe, G. M.; Epstein, L. F. *J. Chem. Phys.* **1956**, *24*, 279.
(26) Akcasu, A. Z. *Polymer* **1981**, *22*, 1169.
(27) Yamakawa, H.; Yoshizaki, T. *J. Chem. Phys.* **1989**, *91*, 7900, and references cited therein.
(28) Koyama, H.; Yoshizaki, T.; Einaga, Y.; Hayashi, H.; Yamakawa, H. *Macromolecules* **1991**, *24*, 932.

Registry No. PS (homopolymer), 9003-53-6.